

Fitting Dynamical Models to Observations of Globular Clusters

Dean E. McLaughlin

*Space Telescope Science Institute, 3700 San Martin Drive, Baltimore,
MD 21218 USA*

Abstract. The basic ingredients of models for the internal dynamics of globular clusters are reviewed, with an emphasis on the description of equilibrium configurations. The development of progressive complexity in the models is traced, concentrating on the inclusion of velocity anisotropy, rotation, and integrals of motion other than energy. Applications to observations of extragalactic globulars and to combined radial-velocity and proper-motion datasets are discussed.

1. Introduction

The dynamical modeling of globular clusters has a long and rich history that intersects repeatedly with fundamental developments in modern astrophysics. A flavour of this history has already been given by G. Meylan in his introduction to this volume, and a fuller account may be found in the review of Meylan & Heggie (1997). In this shorter contribution, it is necessary to omit discussion of a wide range of interesting and important topics, many of which are also covered thoroughly by Meylan & Heggie and updated by other articles in the present proceedings. Thus, the following does not consider any details of the approach of a dense stellar system to a relaxed state, nor indeed any aspect of the “microphysics” of dynamical evolution (evaporation, core collapse and oscillations, the approach to energy equipartition, the role of binaries, three-body encounters, and more). Instead, the focus is on the comparison of dynamical models with only the most basic of cluster observables: surface-brightness profiles and internal stellar velocity distributions along the line of sight and in the plane of the sky. The valuable addition of data on present-day stellar mass functions is also left to other discussions. Even in this already limited context, it is necessary to distinguish between at least three classes of model that are in play.

First is the classic approach pioneered by King (1966a) and Gunn & Griffin (1979) (see also Lupton et al. 1987), in which a static cluster is assumed and a parametric form for the stellar phase-space distribution function (DF) specified at the outset. Basic equations of stellar dynamics are then applied to compute self-consistent spatial densities and velocity moments that can be compared (after projection) to data in order to constrain the parameters of the assumed DF. Although this approach can be restrictive in the sense that it forces a functional form on the DF that might not be appropriate in reality, it is conceptually very well defined, computationally accessible on any desktop computer, and impressively successful. It has been applied, at varying levels of complexity, to almost

every one of the ~ 150 globular clusters in the Milky Way, and to many in other galaxies as well.

Second are non-parametric analyses, which still assume a static equilibrium but begin by constructing smooth and robust functions that describe the observed run of surface brightness and velocity dispersion. Abel-type deprojections are then applied to these to derive the intrinsic density and velocity fields, and an estimate of a phase-space DF whose functional form is dictated more directly by the data (but not completely so, since additional, and restrictive, assumptions—such as velocity isotropy—are always required in the end to extract the DF from deprojected velocities and space densities). These techniques have been applied to only a few individual globulars (e.g., Gebhardt & Fischer 1995; Merritt et al. 1997).

Third, evolutionary models that rely on direct integrations of the Fokker-Planck equation (a second-order approximation to the full, time-dependent statistical mechanical master equation for the stellar DF, which includes the effects of gravitational scattering) can be used to construct a detailed history of a theoretical cluster, and thus a sequence of models vs. time for comparison with observation. This approach is the most physically rich by far of the three, as it allows potentially for the inclusion of much of the detailed microphysics mentioned above. It is computationally intensive, however, and still requires certain assumptions on the underlying stellar dynamics to be made for practical reasons. It has only been applied to a handful of clusters (Drukier et al. 1992; Grabhorn et al. 1992; Drukier 1995; Dull et al. 1997; Giersz & Heggie 2003).

Aside from these established procedures, it should soon be possible to compare still more general and realistic types of models with globular cluster observations; indeed, the amount and variety of surface-brightness, radial-velocity, proper-motion, and mass-function data now becoming available for individual clusters fairly demand it. Adaptations of the orbit-based modeling technique long applied to galaxies (Schwarzschild 1979; Richstone & Tremaine 1984) are promising as a new way to static cluster models that assume nothing *a priori* about the form of the stellar distribution function or the shape of the stellar velocity ellipsoid (e.g., Gebhardt et al. 2002); and direct N -body simulations that require only the input of correct initial conditions to produce star-by-star models of clusters are not far off.

The following discussion reviews some aspects of the first class of models based on parametric prescriptions for the stellar distribution function. This might seem almost old-fashioned in the light of “new horizons” in globular cluster astronomy. But insofar as all models should be expected to fail at some point, progress comes as much from a clear view of their limitations as from their successes. It is also worth bearing in mind that, with the HST, the internal structure of globular clusters outside the Milky Way and beyond the Local Group can now be observed. The relative simplicity of the current and foreseeable data on extragalactic clusters makes them similar in many ways to those that were available for Galactic globulars twenty years ago or more, and the simple models which provided so much insight then are no less useful now.

2. Single-mass, isotropic, lowered isothermal spheres

All modern parametric models of globular clusters are founded in the statistical theory of stellar dynamics developed in the first half of the twentieth century (see, e.g., Spitzer 1987 for a history). A key concept in this connection is the relaxation time, τ_{relax} —the characteristic timescale on which the velocity of a star in a cluster will change by order of itself as a result of gravitational encounters (Spitzer & Hart 1971). The value of τ_{relax} is a function of position in a cluster—it scales fundamentally as σ^3/ρ , where ρ and σ are the density and rms velocity of the stellar field in the cluster—and is commonly evaluated both in the core and at the radius containing half the total cluster light (or mass) in projection. Figure 1 is a histogram of the core and half-mass relaxation times in Galactic globular clusters, taken from Harris’ (1996) online catalogue of cluster properties (see also Djorgovski 1993). This graphically illustrates the well known fact that the inner regions of globular clusters tend to be dynamically relaxed: τ_{relax} there is usually shorter than the age of the systems.

It is worth recalling, however, that this is *not* generally the case in the outer regions of the clusters (von Hörner 1957). If R_h is the projected half-mass radius of a cluster, then—anticipating the fact that an average Galactic globular can be described by a King (1966a) model with a concentration parameter $c \simeq 1.5$ —half the cluster mass is contained in the shell $R_h \lesssim r \lesssim 4R_h$ (still only $\sim 1/3$ of the way to the tidal radius). The average velocity dispersion of stars in this shell is perhaps 75% that of the inner sphere $r \leq R_h$, while the average density of the shell is a factor of 50 lower than that inside $r \leq R_h$. The relaxation time in this outer shell is then $\sim 50 \times (0.75)^3 \approx 20$ times longer than that at the half-mass radius; it becomes comparable to or longer than a Hubble time in most cases.

The importance of relaxation is that it drives the stellar velocity distribution towards a Maxwellian form, $n(v) \propto \exp(-v^2/2\sigma^2)$, and on the basis of Fig. 1 this fact must be reflected in any phase-space distribution function (DF: $f \equiv d^6N/d^3\mathbf{r} d^3\mathbf{v}$) specified as a model for globular clusters. In addition,

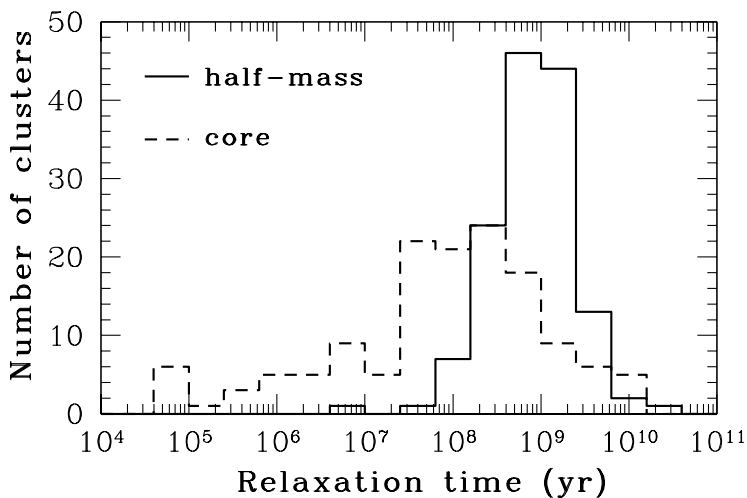


Figure 1. Relaxation times of Galactic globular clusters.

Jeans (1915) and Lynden-Bell (1962a) showed that the DF of a collisionless and steady-state stellar system (one which is described by the collisionless Boltzmann equation, $df/dt = 0$) is a function only of its isolating integrals of motion (those quantities that are conserved along a stellar orbit *and* that work to confine it to a finite volume of phase space). There are at most three isolating integrals for a star moving in three spatial dimensions: its orbital energy E ; one derived from its angular momentum vector \mathbf{L} (e.g., the magnitude L^2 in a spherically symmetric self-gravitating system with an anisotropic velocity ellipsoid; but only the component L_z in an axisymmetric and rotating configuration); and a third (say, I_3) which is calculable in closed form for only a handful of simple gravitational potentials (e.g., Lynden-Bell 1962b; Lynden-Bell 2003).

A third important fact is that a globular cluster moving in the potential of the Galaxy is necessarily limited in its spatial extent by tidal forces. This effect is typically included approximately in models by a simple truncation of the specified DF at high stellar energies corresponding to motion at the escape velocity (though see, e.g., Kashlinsky 1988 and Heggie & Ramamani 1995 for alternate approaches).

These points were brought together in different ways for models of globular clusters by many authors, in a flurry of papers in the 1960s (e.g., Oort & van Herk 1959; Woolley & Dickens 1961; Michie 1961, 1963; Michie & Bodenheimer 1963; King 1965, 1966a; see King 1966a for a review to that point). King's incisive presentation of his particular model in observational terms was a key factor in its dominance throughout the following decades.

King (1966a) assumed a spherical cluster of identical-mass stars with no net streaming motions, and an isotropic velocity ellipsoid so that the only isolating integral of motion is the orbital energy, E [thus, the DF is $f = f(E)$]. With the further impositions of a near-Maxwellian velocity distribution for tightly bound stars ($E \ll 0$) and a tidal cut-off represented by a linear dependence $f \sim -E$ as $E \rightarrow 0$, his model is defined by $f(E) \propto \rho_0 (2\pi\sigma_0^2)^{-3/2} [\exp(-E/\sigma_0^2) - 1]$ for $E = v^2/2 - \phi(r) < 0$ (with $\phi = E = 0$ defining the tidal radius), and by $f(E) \equiv 0$ for all $E \geq 0$. The definition $\rho \equiv \int_0^\infty 4\pi v^2 f(E) dv$ gives $\rho(\phi)/\rho_0$ —the stellar space density, normalized by its central value, as a function of the gravitational potential—and integration of Poisson's equation $d^2\phi/dr^2 + (2/r)d\phi/dr = 4\pi G\rho(\phi)$ gives ϕ/σ_0^2 and then ρ/ρ_0 as functions of a dimensionless radius r/r_0 . This implicit procedure yields the dimensionless tidal radius, r_t/r_0 , at which $\rho = \phi = 0$. It is subject only to the specification of one free boundary condition: the value $W_0 = -\phi(0)/\sigma_0^2$ of the dimensionless potential at the center of the cluster. Finally, the one-dimensional velocity-dispersion profile, σ^2/σ_0^2 , follows from $d(\rho\sigma^2)/dr = -\rho d\phi/dr$.

A single parameter [$W_0 \in (0, \infty)$, or equivalently the concentration parameter $c \equiv \log(r_t/r_0)$] thus serves to specify fully the internal structure of a King (1966a) model in dimensionless form. For comparison with a real cluster, density and velocity profiles as functions of physical radius are obtained by specifying the additional factors ρ_0 , σ_0 , and r_0 [only two of which are independent, since $r_0^2 = 9\sigma_0^2/(4\pi G\rho_0)$ by dimensional analysis of Poisson's equation]. Standard projection integrals applied to these functions yield a directly observable line-of-sight velocity-dispersion profile, $\sigma_z(R)$ and a surface *mass* density profile $\Sigma(R)$ as functions of projected radius R in the plane of the sky. Finally, a mass-to-

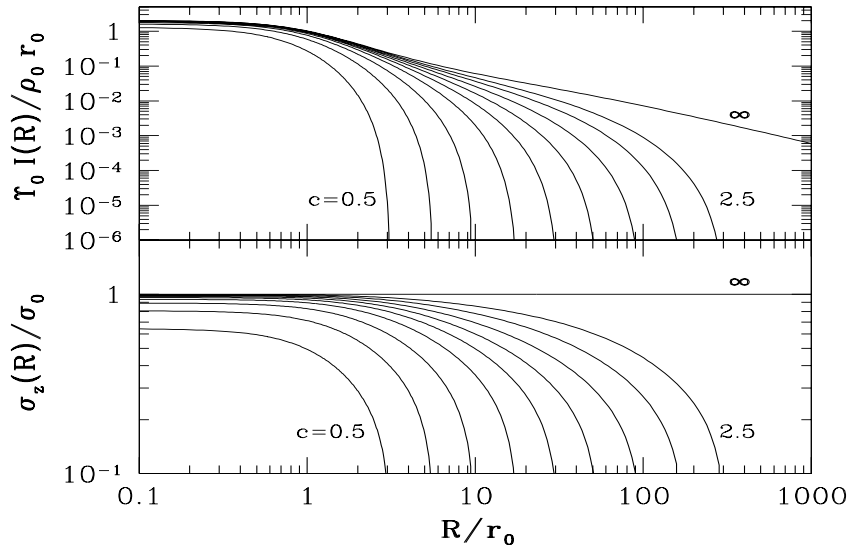


Figure 2. Run of luminosity surface density I and line-of-sight velocity dispersion σ_z vs. projected clustercentric radius R for models from the family of King (1966a). Profile shapes are set by the concentration parameter, $c \equiv \log(r_t/r_0)$, with values shown from $c = 0.5$ to $c = 2.5$ in steps of 0.25. $c = \infty$ corresponds to a Maxwellian DF with no high-energy truncation: an isothermal sphere of infinite spatial extent.

light ratio, Υ_0 (spatially constant under the assumption of a single-mass stellar population), is applied to obtain a model for the observable luminosity surface density profile: $I(R) \equiv \Sigma(R)/\Upsilon_0$. Thus, the fitting of a King(1966) model to data ultimately involves four free parameters to be constrained.

Figure 2 shows (following King 1966a) a grid of dimensionless model profiles in projection. Again, although five different parameters (c , and the four scaling factors) can be counted here, only four are independent given the necessary connection between r_0 , ρ_0 and σ_0 . Evidently, fitting a model intensity profile to an observed one is sufficient to predict the shape of the velocity-dispersion profile, modulo only a normalization linked to Υ_0 . Note also that the velocity scale σ_0 is not the same, in general, as the central velocity dispersion, although the two are close in high-concentration (closely isothermal) models.

It is interesting to consider in slightly more detail the form of the high-energy cut-off in the otherwise Maxwellian DF specified by King (1966a):

$$f(E) \propto \begin{cases} \exp(-E/\sigma_0^2) - 1 & , E < 0 \\ 0 & , E \geq 0 \end{cases} ,$$

which was also adopted by Michie (1963). There is theoretical justification for this particular cut-off—which leads to $f(E) \sim -E$ as $E \rightarrow 0$ —in a relaxed and isolated cluster whose sphericity is unperturbed by tidal forces (King 1965; Spitzer & Shapiro 1971). However (as Fig. 2 illustrates), the exclusion of high-velocity stars from the DF affects the spatial structure in the outer halo of a

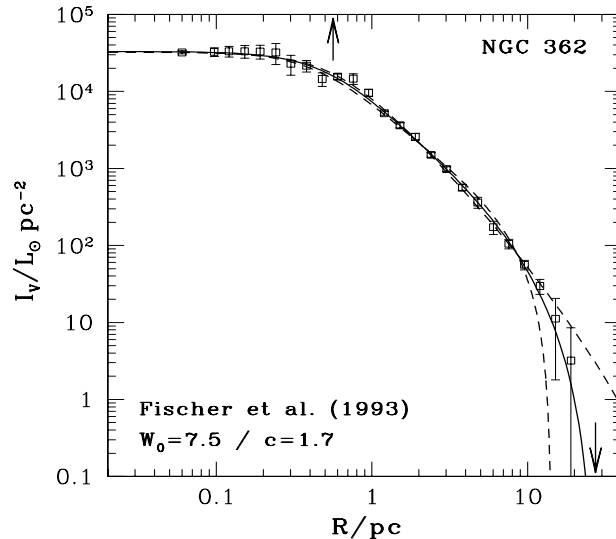


Figure 3. Surface brightness profile of NGC 362, as fit by a King (1966a) model of concentration $c = 1.7$ (solid line). Arrows mark the fitted scale radius r_0 and tidal radius r_t . Dashed curves are best fits of self-consistent surface density profiles corresponding to alternate high-energy truncations of the phase-space distribution function.

model cluster, a region which in real globulars is neither relaxed nor unperturbed by tides. Other simple truncations of a single-mass and isotropic Maxwellian DF have been considered in the literature, such as (among others) the more sudden one of Woolley & Dickens (1961):

$$f(E) \propto \begin{cases} \exp(-E/\sigma_0^2) & , E < 0 \\ 0 & , E \geq 0 \end{cases} ;$$

and the more gradual one of Wilson (1975):

$$f(E) \propto \begin{cases} \exp(-E/\sigma_0^2) + E/\sigma_0^2 - 1 & , E < 0 \\ 0 & , E \geq 0 \end{cases} ,$$

which gives $f(E) \sim E^2$ as $E \rightarrow 0$.

King (1966a) himself considered each of these alternate energy truncations. He compared the self-consistent surface-density profiles they predict with observed star-counts in the halo of M13 and concluded that the data were most consistent with the linear dependence on E in the high-energy tail of his DF. Figure 3 illustrates this for a different—and by all appearances thoroughly average—cluster, NGC 362 (data from Fischer et al. 1993). The curves, from top to bottom in the right-hand corner of the graph, correspond to best fits of Wilson’s (1975) DF, King’s (1966a) DF, and Woolley & Dickens’ (1961) DF. The standard model is clearly favored, but the conclusion rests entirely on data from the outermost, least relaxed and least “isolated” parts of the cluster. In cases where a regular King model might *not* provide a perfect description of a surface-brightness profile (and there are many such cases), it must be remembered that

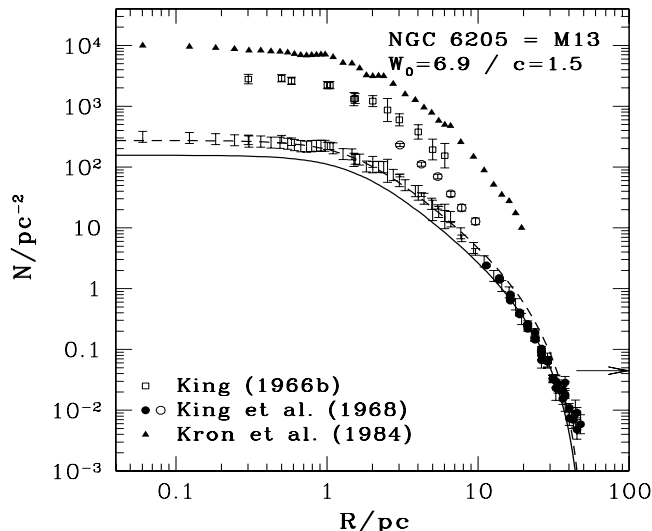


Figure 4. Combination of data defining the current empirical surface density of M13 (NGC 6205). King (1966a) models plotted both have $c = 1.5$, but different density normalizations and scale radii r_0 .

the shape of the model profile depends not only on the explicit assumptions of isotropy and equal-mass stars, but also on the implicit assumptions [through the linear dependence of $f(E)$ near the escape energy] of relaxation and isolation in the extreme halo.

King and collaborators collected and fit surface-density data, in the form of star counts and integrated surface-brightness measurements, for scores of globular clusters (King 1966b; King et al. 1968). This database was enlarged by other important surveys over the next twenty years (notably, e.g., Illingworth & Illingworth 1976; Kron et al. 1984). All such studies were most recently compiled by Trager et al. (1995), who combined often overlapping data to define a single, calibrated surface-brightness profile and a smooth interpolation curve for each of 125 Galactic globulars. The example of M13 is illustrated in Fig. 4. Star counts by King et al. (1968) in the outer regions of the cluster define the vertical scale of the graph; another set of inner star counts, and two sets of photoelectric surface-photometry measurements, are shown with arbitrary offsets for clarity. To construct a continuous surface-density profile, the inner star counts and photometry are scaled first to agree with each other, and then (as indicated by the errorbars with no symbols) to provide the best match in the (small!) region of overlap with the outer star counts. Shown as a solid line is the model that King (1966a) found as the best fit in the outer parts of M13; the dashed curve is the best fit including the inner data.

Clearly, a King model in this case is not the perfect fit found in NGC 362. The horizontal arrow at the right of the Figure indicates the level of background contamination in the star counts of King et al. (1968), as a reminder that the observational definition of $I(R)$ is most prone to error in the outermost regions of the cluster that, as in Fig. 3, are often the most influential in accepting or rejecting an overall class of dynamical model. While this caveat must be borne

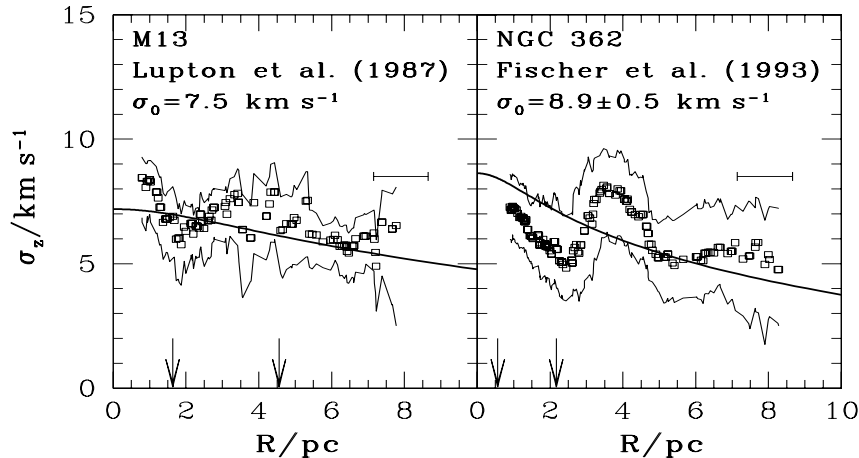


Figure 5. Line-of-sight velocity-dispersion profiles in M13 and NGC 362, compared with single-mass, isotropic, King(1966) model curves corresponding to the surface-density fits in Figs. 4 and 3. Arrows mark the fitted scale radius r_0 and projected half-light radius R_h .

in mind, a more positive aspect of this plot—which is fairly representative of the profiles collected by Trager et al. (1995)—is the verification that a standard King model is nevertheless an excellent first-order approximation to the spatial structure of an average globular cluster. The difference between the solid and dashed curves can be viewed as an indication of the typical uncertainties in King-model fitting, which are discussed fully by Trager et al. (1995). An up-to-date catalogue of the structural parameters fitting the clusters of Trager et al., and some 20 others, is maintained online by W. E. Harris (Harris 1996).

It took somewhat longer for high-quality radial velocities to become available for comparison with the predicted kinematics of single-mass, isotropic King models (lower panel of Fig. 2). Illingworth (1976) obtained integrated-light spectra of the cores of 10 globulars to estimate their central velocity dispersions and thence (by referring to surface-brightness fits of a King model) mass-to-light ratios. In terms of direct dynamical tests, Da Costa et al. (1977) fit models simultaneously to surface brightness and the velocities of 11 individual giants in NGC 6397, while Gunn & Griffin (1979) used radial velocities of 111 giants together with a surface-brightness profile in M3 to show the need for a multi-mass and anisotropic generalization of the King model. Their paper opened the floodgates for such data and analyses (see Meylan & Heggie 1997 for a complete listing of the subsequent work), and some 15 years later Pryor & Meylan (1993) were able to summarize velocity information on 56 Galactic globulars. This remains the most recent such compilation. The sizes of radial-velocity samples in individual globulars have since grown steadily, reaching now into the thousands for several clusters.

Figure 5 shows spatially smoothed velocity-dispersion profiles of M13 and NGC 362, constructed from the data published in Lupton et al. (1987) and Fischer et al. (1993), by robustly estimating the rms velocity of all stars falling within an annulus of fixed width (indicated by the horizontal errorbars in the Figure) as it is centered on every star in turn. The jagged lines in the panel for

M13 indicate 1- σ uncertainties; those in the NGC 362 panel, 2- σ uncertainties. The curves are the predicted σ_z profiles for the King (1966a) models fit to the surface brightnesses in Figs. 3 and 4, with a normalization σ_0 corresponding in each case to a V-band mass-to-light ratio $\Upsilon_0 \simeq 1.5 M_\odot L_\odot^{-1}$. The basic, *first-order* confirmation of the model, in Figs. 3, 4, and 5 combined, is impressive. However, both Lupton et al. (1987) and Gebhardt & Fischer (1995) conclude through more detailed analyses of these data—and studies of similar and better datasets in other clusters also indicate—that non-trivial modifications of King’s single-mass and isotropic assumptions are necessary.

3. Structural correlations, the fundamental plane, and extragalactic globulars

Before outlining the necessary modifications to King (1966a), the general success of that theory provides an excellent opportunity to construct a uniform view of the gross structure and internal dynamics of globular clusters. In particular, the multitude of correlations between fitted King-model parameters, and any number of physical quantities derived from them (Djorgovski & Meylan 1994; Djorgovski 1995; Djorgovski, this volume), offer deep insight into questions of cluster formation and evolution.

Figure 6 shows the two strongest correlations known for Galactic globulars with central velocity-dispersion measurements (Djorgovski 1995). The scatter in these correlations is entirely due to measurement errors, and they define a fundamental plane analogous to, but significantly different from, that of elliptical galaxies. The label “plane” in this case is entirely accurate since single-mass,

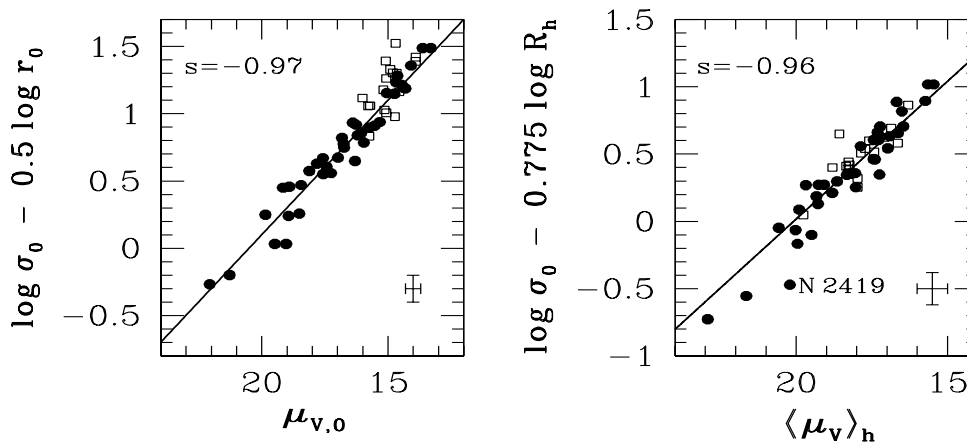


Figure 6. One representation of the fundamental plane of Galactic globular clusters (cf. Djorgovski 1995). Solid line in the left panel is the equation of a uniform mass-to-light ratio $\Upsilon_{V,0} \equiv 1.45 M_\odot L_{V,\odot}^{-1}$ for single-mass, isotropic King-model clusters, as derived by McLaughlin (2000a). That in the right panel is the equation $E_b = 6.6 \times 10^{39} \text{ erg } (L/L_\odot)^{2.05}$, from McLaughlin (2000a). Open squares represent core-collapsed clusters.

isotropic King models have exactly four free parameters (§2); thus, insofar as real clusters can be considered realizations of these models, they could in principle occupy the whole of a four-dimensional space. The existence of two independent correlations restricting their physical properties instead confines them to a two-dimensional surface inside this larger space. (In Fig. 6, five different structural parameters are indicated, but a theoretical King model can always be used to derive any one of these in terms of the other four.)

Any four quantities can be taken as a physical basis to define the family of King (1966a) models, so long as they are mutually independent; any two such sets of variables can be shown to be equivalent, and the choice of which to work with is an issue only of convenience or preference. McLaughlin (2000a) takes the independent cluster properties to be total luminosity L , mass-to-light ratio Υ_0 , global binding energy E_b , and concentration $c = \log(r_t/r_0)$. He then shows directly that all non-core-collapsed clusters share a common $\Upsilon_0 = 1.45 M_\odot L_\odot^{-1}$ in the V band, and obey a strict scaling between total binding energy, luminosity, and galactocentric position: $E_b = 7.2 \times 10^{39} \text{ erg } (L/L_\odot)^{2.05} (r_{\text{gc}}/8 \text{ kpc})^{-0.4}$. McLaughlin further shows how the correlations in Fig. 6—and all others between any other cluster properties—derive directly from these constraints on Υ_0 and E_b if all clusters are assumed to be accurately described by single-mass, isotropic King models. This is the the physical significance of the fundamental plane.

It is now also possible to fit isotropic King models to extragalactic globular clusters, and those in M31 (Djorgovski et al. 1997; Barmby et al. 2002), NGC 5128 (Harris et al. 2002), and M33 (Larsen et al. 2002) have been found to lie on essentially the same fundamental plane as those in the Milky Way. The apparently typical scaling between global energy and luminosity or mass, $E_b \sim L^2 \propto M^2$, is nontrivial, and understanding it will be important in developing a comprehensive theory of star and cluster formation (McLaughlin 2000b).

4. Multiple stellar masses, velocity anisotropy, and rotation

Despite its substantial successes, the simple model of King (1966a) inevitably showed some cracks when data of very high quality began to accumulate. Figure 7 shows the surface-density profile of M3, as traced by a combination of star counts and appropriately normalized surface photometry. The two solid curves are single-mass, isotropic King models of two different concentrations, which separately describe the inner and outer structure of this cluster. No single such model is capable of reproducing the full density profile (as the dashed curve, of concentration intermediate to the inner and outer fits, suggests).

This point was first made by Da Costa & Freeman (1976), who suggested that the problem could be resolved if stars of different masses (say m_i and m_j) had different velocity dispersions at a given radius, in accordance with energy equipartition ($m_i \sigma_i^2 = m_j \sigma_j^2$). They continued to assume velocity isotropy, and therefore specified a model distribution function as

$$f(E) = \sum f_i \quad , \quad f_i = C_i \left[\exp(-E/\sigma_{i,0}^2) - 1 \right] \quad (E < 0) \quad .$$

(Oort & van Herk 1959 also constructed a multimass model for M3, but with a sharp truncation of the DF at high energies as in Woolley & Dickens 1961.)

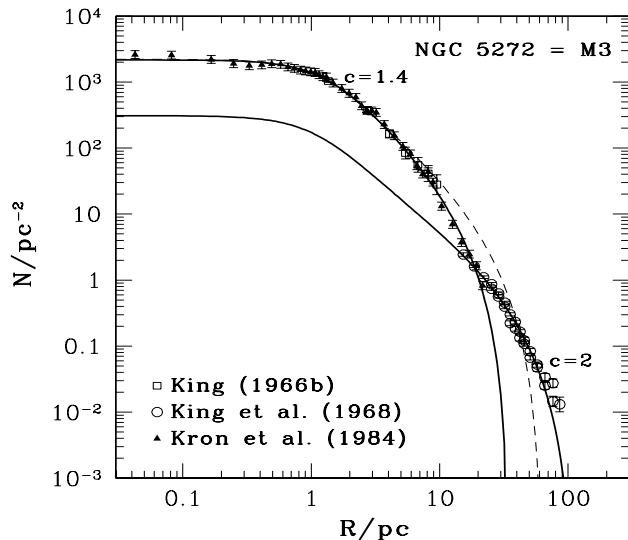


Figure 7. Failure of a single King (1966a) model to fit the spatial structure of M3 (NGC 5272). After Da Costa & Freeman (1976).

The relative numbers of stars in each of several discrete mass bins—i.e., the values of the coefficients C_i —were set by extrapolation of the observed stellar luminosity function, allowing the construction of a self-consistent model that fit the surface-density profile in Fig. 7 well. The allowance of energy equipartition imparts a larger-than-average velocity dispersion to low-mass stars, thus providing a greater number of stars on high-energy orbits and an excess population (relative to the original King model) of the halo regions of the cluster.

Gunn & Griffin (1979) revisited M3 with radial velocities for 111 cluster members also in hand. They argued for a much different extrapolation of the observed stellar luminosity function and substantially different relative mass-class populations than Da Costa & Freeman specified. In this case, they found it impossible to fit both the surface-brightness profile and the line-of-sight velocity distribution while keeping the assumption of isotropy. They continued to assume spherical symmetry (no net rotation) and defined a “Michie-King” model by a DF depending on two isolating integrals: E , and the magnitude L^2 of the specific angular-momentum vector to allow for velocity anisotropy:

$$f(E, L) = \sum f_i \quad , \quad f_i = C_i \exp\left(-L^2/2\sigma_{i,0}^2 r_a^2\right) \left[\exp\left(-E/\sigma_{i,0}^2\right) - 1\right] \quad (E < 0) \quad .$$

In the limit $r_a \rightarrow \infty$, this DF reduces to that of Da Costa & Freeman; and from that, to the standard King (1966a) form. More generally, the functional dependence on L^2 in this DF (which was also adopted by Michie 1963 and appears in Eddington’s 1915 distribution function) provides for approximate velocity isotropy inside the sphere $r \lesssim r_a$ and a radial bias in the velocity ellipsoid that increases toward larger radii. Aside from this, there is no theoretical motivation for the specific term $e^{-L^2/(2\sigma_{i,0}^2 r_a^2)}$; it is much more *ad hoc* than the form of the high-energy truncation.

Gunn & Griffin fit all the available data in M3 by a model with r_a comparable to the cluster’s projected half-light radius, consistent with the idea of velocity

isotropization by relaxation inside that radius. The prediction of a radial velocity anisotropy in the outer parts of the cluster is untested. Meanwhile, it has become routine to fit surface-brightness and radial-velocity data simultaneously with Michie-King models, owing in part to their early application by Pryor and collaborators (e.g., Pryor et al. 1986) and by Meylan (1987, 1988). Typically, good fits to all available data can be achieved—hardly surprising given the number of variables in the models. In fact, the effects of an increase in the relative population of low-mass stars can mimic those of a more strongly radially biased velocity ellipsoid, such that several physically different models can often fit the same dataset equally well.

It is notable that Michie-King fits tend to be constrained more by features in the surface-brightness profiles (inflection points, or convexity in the outer regions) than by the radial-velocity dispersion profiles (which generally do not stray far from their overall behavior in the isotropic models of Fig. 2). The obvious danger of inferring velocity anisotropy largely from surface photometry (or perhaps the inadequacy of the anisotropy term in the Michie-King distribution function) has been illustrated in ω Centauri. Merritt et al. (1997) analyzed, with non-parametric techniques, the same data that Meylan et al. (1995) used to fit Michie-King models to this cluster. Whereas the Meylan et al. model fits require strong radial anisotropy setting in at just under a half-mass radius, Merritt et al. assumed isotropy throughout the entire cluster and were able to find a self-consistent DF that could account for all structural and kinematic data.

The assumption of strict equipartition of energy in these models may also be questionable, as there are physical scenarios in which multimass populations of stars in a hydrostatic equilibrium configuration can *not* be in thermal equilibrium (Spitzer 1969; Lightman & Fall 1978; Kondrat'ev & Ozernoy 1982). Michie-King models can provide more acceptable fits than King (1966a) models given a wider range of more detailed data in a globular cluster, but at the cost of introducing more free parameters under more tenuous physical assumptions.

The discovery of significant rotation in some globular clusters (e.g., 47 Tucanae and ω Centauri: Meylan & Mayor 1986; M13: Lupton et al. 1987; and more than 10 others since with v_{rot}/σ ranging from ~ 0.01 to 0.5) further complicates matters. To take proper account of rotation, axisymmetry is assumed instead of spherical symmetry, and the isolating integrals of motion in the stellar DF are E and the component L_z of angular momentum along the rotation axis. If arbitrary velocity anisotropy is to be allowed, then the (generally unknown) third integral must also appear explicitly: $f = f(E, L_z, I_3)$. And given only radial-velocity data, the inclination of the cluster to the plane of the sky automatically becomes another free parameter. Despite these difficulties, Lupton & Gunn (1987) developed parametric models of multimass, anisotropic, rotating and flattened clusters by first using L^2 as a (very crude) approximation to I_3 , and then multiplying every component of the Michie-King DF by a term of the (*ad hoc*) form $e^{\gamma L_z}$. Lupton et al. (1987) were able to fit such models to the surface brightness and radial velocities in M13, given also some internal proper motions and the observed stellar mass function there; but the many enhancements over King's (1966a) model are again constrained far more strongly by the surface-brightness profile than by any velocity data (recall Fig. 5 above, which shows the σ_z profile in M13 to be fully consistent with velocity isotropy).

Even with a maximum of approximation and assumption, parametric modeling at this level of detail is almost prohibitively complex, and the rotating model of Lupton & Gunn (1987) has not been applied to any cluster other than M13. But given the wealth of cluster dynamical data available now and coming in the near future (large proper-motion samples; high-quality stellar luminosity functions) it seems inescapable that accurate two- and three-integral, multi-mass models will need to be developed. It may be possible to develop useful parametric, DF-based models by retaining a reduction to some type of lowered Maxwellian in the appropriate limits but drawing on the vast literature of galaxy models for revised treatments of velocity anisotropy and third integrals. However this might play out, more numerical methods—orbit integrations along the lines of Schwarzschild (1979), anisotropic Fokker-Planck simulations (Takahashi 1997; Drukier et al. 1999; Takahashi & Portegies Zwart 2000), or direct N -body simulations—will necessarily take on new importance.

5. Proper motions

The use of internal proper motions in dynamical models has been understandably more limited than the application of line-of-sight velocities: a linear velocity dispersion of 10 km s^{-1} or less in a (crowded) cluster core corresponds, at a heliocentric distance of 8 kpc, to a dispersion of $\lesssim 0.25 \text{ mas yr}^{-1}$ in proper motion. Large datasets with time baselines long enough and internal errors small enough to resolve such motion—let alone trace its variation with clustercentric radius—are not easily come by from the ground. Notable efforts by Cudworth and collaborators (e.g., Cudworth 1976a, 1976b, 1979; Peterson & Cudworth 1994) allowed for basic velocity-dispersion estimates and astrometric distance determinations in a handful of clusters. Leonard & Merritt (1989) and Leonard et al. (1992) used limited proper-motion data (comparable to the earliest radial-velocity data) to constrain Jeans-equation mass estimates of M35 and M13, while Lupton et al. (1987) compared their DF-based model of M13 with the sparse proper motions available there.

A substantial breakthrough has come recently, both with the publication of a huge set of ground-based proper motions for nearly 8000 stars in ω Centauri by van Leeuwen et al. (2000), and with the application of new techniques for space-based astrometry with HST to obtain tens of thousands of proper motions in ω Centauri and 47 Tucanae (see King & Anderson 2001, 2002; Anderson, these proceedings; and the poster of McLaughlin et al. in this volume for reports on preliminary results). The potential of these data to constrain any kind of detailed dynamical model is immense, but they have not yet been fully exploited.

Just one taste of the wealth of information contained in proper motions is provided by Fig. 8, using the data of van Leeuwen et al. (2000) for ω Centauri. Plotted there is the ratio of the plane-of-sky velocity dispersion in the direction along the projected radial vector from the center of the cluster (σ_R) to that in the projected azimuthal direction (σ_Θ). In a spatial average, and under the assumptions of spherical symmetry and no net rotation (both of which are, strictly, incorrect here), this ratio is related to the ratio of unprojected radial and tangential velocity dispersions, σ_r/σ_θ , by (Leonard & Merritt 1989)

$$2 \sigma_r^2 / \sigma_\theta^2 = 3 \sigma_R^2 / \sigma_\Theta^2 - 1 .$$

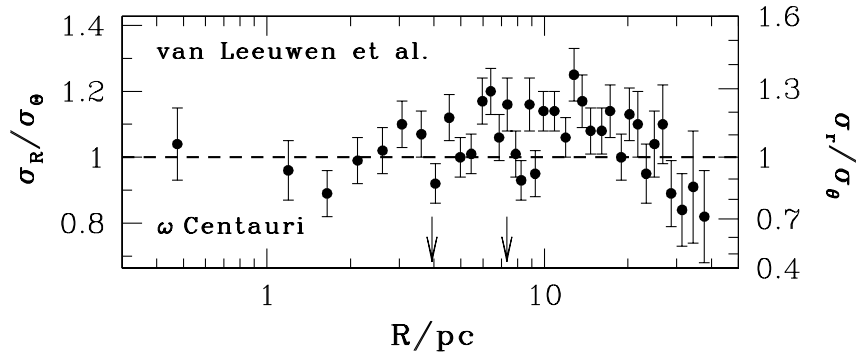


Figure 8. Ratio of radial and tangential velocity dispersions on the plane of the sky in ω Centauri (NGC 5139), and the corresponding unprojected quantity, as a direct measure of velocity anisotropy. The King-model scale radius and projected half-light radius are indicated.

While this particular relation is not completely general, it is clear that the usual velocity anisotropy parameter, $\beta \equiv 1 - \sigma_\theta^2/\sigma_r^2$, can be deduced directly from proper-motion dispersions. These data specifically appear to confirm that the strong radial anisotropy inferred to obtain outside a half-light radius in ω Centauri (cf. §4) according to fits of parametric Michie-King models, may be more an artifact of the model construction than a physical effect (see also King & Anderson 2002).

The signature of rotation in proper motions can also be used to estimate directly the inclination of an axisymmetric cluster, and to delineate empirically the form of a (non-solid-body) rotation field (e.g., van Leeuwen et al. 2000). Wybo & Dejonghe (1995, 1996) and Heacox (1997, 1998) give much more detailed theoretical discussions on the extraction of dynamical information from proper-motion datasets. Further development of these and similar tools, both to mesh them with the new, high-quality data and to extend them to apply to general gravitational potentials and arbitrary stellar distribution functions, presents an important challenge.

References

- Barmby, P., Holland, S., & Huchra, J. P. 2002, *AJ*, 123, 1937
 Cudworth, K. M. 1976a, *AJ*, 81, 519
 Cudworth, K. M. 1976b, *AJ*, 81, 975
 Cudworth, K. M. 1979, *AJ*, 84, 1312
 Da Costa, G. S., & Freeman, K. C. 1976, *ApJ*, 206, 128
 Da Costa, G. S., Freeman, K. C., Kalnajcs, A. J., Rodgers, A. W., Stapinsky, T. E. 1977, *AJ*, 82, 810
 Djorgovski, S. 1993, in *ASP Conf. Ser. 50, Structure and Dynamics of Globular Clusters*, ed. S. G. Djorgovski and G. Meylan (San Francisco: ASP), p. 373
 Djorgovski, S. 1995, *ApJ*, 438, L29

- Djorgovski, S., & Meylan, G. 1994, *AJ*, 108, 1292
- Djorgovski, S., Gal, R. R., McCarthy, J. K., et al. 1997, *ApJ*, 474, L19
- Drukier, G. A., Fahlman, G. G., & Richer, H. B. 1992, *ApJ*, 386, 106
- Drukier, G. A. 1995, *ApJS*, 100, 347
- Drukier, G. A., Cohn, H. N., Lugger, P. M., & Yong, H. 1999, *ApJ*, 518, 233
- Dull, J. D., Cohn, H. N., Lugger, P. M., et al. 1997, *ApJ*, 481, 267
- Eddington, A. S. 1915, *MNRAS*, 75, 366
- Fischer, P., Welch, D. L., Mateo, M., & Côté, P. 1993, *AJ*, 106, 1508
- Gebhardt, K., & Fischer, P. 1995, *AJ*, 109, 209
- Gebhardt, K., Rich, R. M., & Ho, L. C. 2002, *ApJ*, 578, L41
- Giersz, M., & Heggie, D. 2003, *MNRAS*, in press ([astro-ph/0210446](#))
- Grabhorn, R. P., Cohn, H. N., Lugger, P. M., & Murphy, B. W. 1992, *ApJ*, 392, 86
- Gunn, J. E., & Griffin, R. F. 1979, *AJ*, 84, 752
- Harris, W. E. 1996, *AJ*, 112, 1487
- Harris, W. E., Harris, G. L. H., Holland, S. T., & McLaughlin, D. E. 2002, *AJ*, 124, 1435
- Heacox, W. D. 1997, *ApJ*, 490, 263
- Heacox, W. D. 1998, *ApJS*, 114, 121
- Heggie, D. C., & Ramamani, N. 1995, *MNRAS*, 272, 317
- Illingworth, G. 1976, *ApJ*, 204, 73
- Illingworth, G., & Illingworth, W. 1976, *ApJS*, 30, 227
- Jeans, J. H. 1915, *MNRAS*, 76, 71
- Kashlinsky, A. 1988, *ApJ*, 325, 566
- King, I. R. 1965, *AJ*, 70, 376
- King, I. R. 1966a, *AJ*, 71, 64
- King, I. R. 1966b, *AJ*, 71, 276
- King, I. R., & Anderson, J. 2001, in *ASP Conf. Ser. 228, Dynamics of Star Clusters and the Milky Way*, ed. S. Deiters, B. Fuchs, R. Spurzem, A. Just, and R. Wielen (San Francisco: ASP), p. 19
- King, I. R., & Anderson, J. 2002, in *ASP Conf. Ser. 265, ω Centauri: A Unique Window into Astrophysics*, ed. F. van Leeuwen, J. Hughes, and G. Piotto (San Francisco: ASP), p. 21
- King, I. R., Hedemann, E., Hodge, S. M., & White, R. E. 1968, *AJ*, 73, 456
- Kondrat'ev, B. P., & Ozernoy, L. M. 1982, *Ap&SS*, 84, 431
- Kron, G. E., Hewitt, A. V., & Wasserman, L. H. 1984, *PASP*, 96, 198
- Larsen, S. S., Brodie, J. P., Sarajedini, A., & Huchra, J. P. 2002, *AJ*, 124, 2615
- Leonard, P. J. T., & Merritt, D. 1989, *ApJ*, 339, 195
- Leonard, P. J. T., Richer, H. B., & Fahlman, G. G. 1992, *AJ*, 104, 2104
- Lightman, A. P., & Fall, S. M. 1978, *ApJ*, 221, 567
- Lupton, R. H., & Gunn, J. E. 1987, *AJ*, 93, 1106
- Lupton, R. H., Gunn, J. E., & Griffin, R. F. 1987, *AJ*, 93, 1114

- Lynden-Bell, D. 1962a, MNRAS, 124, 1
Lynden-Bell, D. 1962b, MNRAS, 124, 95
Lynden-Bell, D. 2003, MNRAS, 338, 208
McLaughlin, D. E. 2000a, ApJ, 539, 618
McLaughlin, D. E. 2000b, in 33rd ESLAB Symposium, Star Formation from the Small to the Large Scale, ed. F. Favata, A. Kaas, and A. Wilson (Noordwijk: ESA), p. 77 ([astro-ph/0002087](#))
Merritt, D., Meylan, G., & Mayor, M. 1997, AJ, 114, 1074
Meylan, G. 1987, A&A, 184, 144
Meylan, G. 1988, A&A, 191, 215
Meylan, G., & Heggie, D. 1997, A&AR, 8, 1
Meylan, G., & Mayor, M. 1986, A&A, 166, 122
Meylan, G., Mayor, M., Duquenois, A., & Dubath, P. 1995, A&A, 303, 761
Michie, R. W. 1961, ApJ, 133, 781
Michie, R. W. 1963, MNRAS, 125, 127
Michie, R. W., & Bodenheimer, P. H. 1963, MNRAS, 126, 267
Oort, J. H., & van Herk, G. 1959, Bull. Astron. Inst. Netherlands, 14, 299
Peterson, R. C., & Cudworth, K. M. 1994, ApJ, 420, 612
Pryor, C., & Meylan, G. 1993, in ASP Conf. Ser. 50, Structure and Dynamics of Globular Clusters, ed. S. G. Djorgovski & G. Meylan (San Francisco: ASP), p. 357
Pryor, C., McClure, R. D., Fletcher, J. M., Hartwick, F. D. A., & Kormendy, J. 1986, AJ, 91, 546
Richstone, D. O., & Tremaine, S. 1984, ApJ, 286, 27
Schwarzschild, M. 1979, ApJ, 232, 236
Spitzer, L. 1969, ApJ, 158, L139
Spitzer, L. 1987, Dynamical Evolution of Globular Clusters (Princeton: Princeton University Press)
Spitzer, L., & Hart, M. H. 1971, ApJ, 164, 399
Spitzer, L., & Shapiro, S. L. 1971, ApJ, 173, 529
Takahashi, K. 1997, PASJ, 49, 547
Takahashi, K., & Portegies Zwart, S. F. 2000, ApJ, 535, 759
Trager, S. C., King, I. R., & Djorgovski, S. 1995, AJ, 109, 218
van Leeuwen, F., Le Poole, R. S., Reijns, R. A., Freeman, K. C., & de Zeeuw, P. T. 2000, A&A, 360, 472
von Hörner, S. 1957, ApJ, 125, 451
Wilson, C. P. 1975, AJ, 80, 175
Woolley, R., & Dickens, R. J. 1961, Royal Greenwich Obs. Bull. No. 42
Wybo, M., & Dejonghe, H. 1995, A&A, 295, 347
Wybo, M., & Dejonghe, H. 1996, A&A, 312, 649